

## APERTURE SYNTHESIS IMAGING OF PARTIALLY IONIZED GAS IN W48

JOSEPH S. ONELLO<sup>1</sup>

Department of Physics, State University of New York, Cortland, NY 13045

J. A. PHILLIPS

Owens Valley Radio Observatory, Caltech 105-24, Pasadena, CA 91125

P. BENAGLIA<sup>2</sup> AND W. M. GOSS

National Radio Astronomy Observatory, Very Large Array, Socorro, NM 87801

AND

YERVANT TERZIAN

Department of Astronomy, Cornell University, Ithaca, NY 14853

*Received 1993 July 20; accepted 1993 November 2*

## ABSTRACT

We present the results of VLA observations of cool gas surrounding the H II region W48 at the H168 $\alpha$  and C168 $\alpha$  transition frequencies. Previous single-dish observations of W48 showed that the 168 $\alpha$  recombination spectrum was composed of a broad line from ionized hydrogen (H<sup>+</sup>) within the H II region, as well as strong, narrow lines (H<sup>0</sup>, C<sup>+</sup>, and S<sup>+</sup>) from gas outside the Strömgen sphere. High spatial resolution imaging of W48 reveals that the strong C<sup>+</sup> and S<sup>+</sup> lines arise from the stimulated amplification of the background H II region. Like the C<sup>+</sup> and S<sup>+</sup> lines, the narrow line from partially ionized hydrogen (H<sup>0</sup>) is strongest near the continuum peak of the H II region and suggests stimulated amplification of the line. The width of the H<sup>0</sup> line constrains the temperature of the partially ionized medium to be less than 200 K. However, the gas in which the H<sup>0</sup> line originates is found not to be spatially coincident with the carbon-emitting region. We suggest that the H<sup>0</sup> emission arises in the advancing ionization front of the H II region, while the C<sup>+</sup> and S<sup>+</sup> lines originate in a more extended region of the ambient molecular cloud partially ionized by photons with  $\lambda > 912$  Å escaping the boundary of the Strömgen sphere.

*Subject headings:* H II regions — ISM: individual (W48) — radio lines: ISM

## 1. INTRODUCTION

In 1990 we observed an unusual set of radio recombination lines (RRLs) from the H II region W48 (Onello, Phillips, & Terzian 1991, hereafter Paper I). Single-dish observations with the Arecibo radio telescope ( $\theta_{\text{res}} \approx 3/2$ ) showed that the H168 $\alpha$  line was composed of two components: a broad line ( $\Delta V \sim 30$  km s<sup>-1</sup>) from hot gas in the fully ionized H II region, and a narrow line ( $\Delta V \sim 5$  km s<sup>-1</sup>) from cold gas lying outside the Strömgen sphere. We also observed narrow recombination lines from singly ionized carbon and a heavier element or blend of heavy elements. Silverglate (1984) tentatively identified the heavy element feature as sulfur. The velocities of the H<sup>0</sup>, C<sup>+</sup>, and S<sup>+</sup> lines were offset by a few km s<sup>-1</sup> from that of the H<sup>+</sup> line, but closely matched the velocity of the CO emission from the ambient molecular cloud. The narrow lines apparently arise in a partially ionized interface between the H II region and the adjacent molecular cloud.

The origin and excitation of the narrow lines are still not understood. Carbon and sulfur have ionization potentials less than hydrogen (11.3 and 10.4 eV, respectively). Carbon and sulfur in cold gas outside the H II region are probably ionized by photons with energies between 10.4 and 13.6 eV which escape the Strömgen sphere. The narrow carbon lines are particularly strong. Although the cosmic abundance of carbon is only  $[C/H] \approx 4 \times 10^{-4}$ , the integrated intensity of the

carbon recombination line is 1/10 that of the hydrogen line. The lines may be very strong because the carbon gas is cold (peak recombination line temperatures scale as  $T^{-1.15}$  in LTE) or their intensities may be enhanced by stimulated emission. If stimulated emission is important we would expect the carbon line to be strongest at the continuum peak of the H II region. We were unable in Paper I to verify this hypothesis because of the limited angular resolution of the Arecibo telescope.

The source for ionization of cold hydrogen is more controversial than that of carbon. One possibility is that the H<sup>0</sup> line is formed in a partially ionized layer at the boundary of the expanding ionization front (Hill 1977), or the gas could be ionized by soft X-rays produced by the hot stellar wind of the ionizing star (Krüger & Tenorio-Tagle 1978). In the former case the cold hydrogen would be localized at the boundary of the H II region, while in the latter the distribution of the ionized gas would be more extended. To investigate the excitation conditions and spatial distribution of partially ionized gas around the W48 H II region we have made an aperture synthesis image of the region in the 168 $\alpha$  RRL transition using the VLA at  $\lambda_{22}$  cm. We detected hydrogen, carbon, and heavy element RRLs from the main source, W48A, and hydrogen RRLs from three other H II regions of the W48 complex. We describe the observations and report our results in §§ 2 and 3, and discuss our findings and conclusions in §§ 4 and 5.

## 2. OBSERVATIONS

We observed W48 at the H168 $\alpha$  (1374.6 MHz) and C168 $\alpha$  (1375.3 MHz) transitions in a single 10 hr run 1992 August 8

<sup>1</sup> Visiting Professor, Department of Astronomy, Cornell University.

<sup>2</sup> Facultad de Ciencias Astronomicas y Geofisicas, Universidad Nacional de La Plata, Argentina.

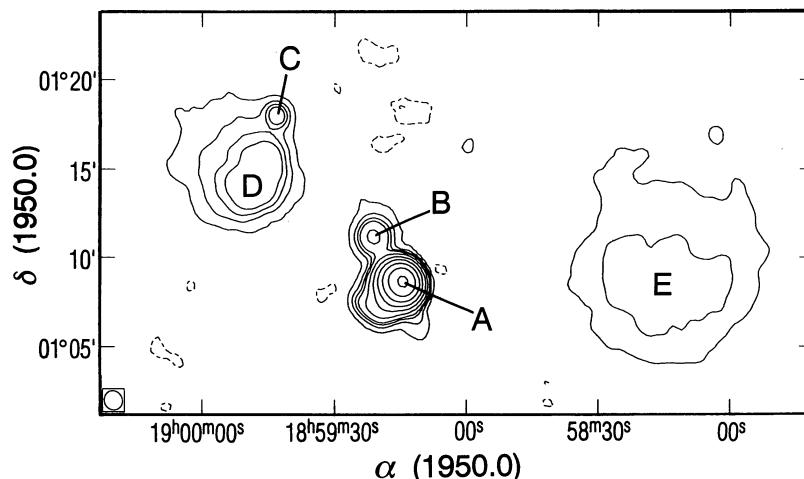


FIG. 1.—1374 MHz continuum map of the W48 H II region complex. Contour levels are  $-15$ ,  $+15$ ,  $45$ ,  $75$ ,  $105$ ,  $187.5$ ,  $375$ ,  $750$  mJy,  $1.5$  Jy,  $3.0$  Jy,  $6.0$  Jy. The lowest positive contour corresponds to  $3\sigma$ .

using the compact D-configuration of the VLA.<sup>3</sup> The synthesized beam was  $66'' \times 61''$  (position angle  $27^\circ$ ) and the H168 $\alpha$  and C168 $\alpha$  lines were centered at a VLSR of  $45 \text{ km s}^{-1}$ . The total bandwidth for the observation was  $0.78125 \text{ MHz}$ . Two IFs with right circular polarization were used resulting in 256 spectral channels for each IF with a frequency separation of  $3.052 \text{ kHz}$  (with a resultant resolution of  $0.8 \text{ km s}^{-1}$ ). The flux density scale was set with the calibrator 3C 286 ( $1328 + 307$ ), while the amplitude and phase were calibrated by interleaving observations of 1923+210 with observations of W48. We observed W48 for 355 minutes and the bandpass calibrator 3C 295 ( $1409 + 524$ ) with a flux density of  $21 \text{ Jy}$  for 120 minutes.

For both the hydrogen and carbon transitions, continuum emission was removed in the visibility data by subtracting from each channel an average of the line-free channel visibilities using the AIPS (Astronomical Image Processing System) routine UVLIN (Cornwell et al. 1992). Two-hundred-fifty-six CLEANed line images were formed by Fourier transforming the visibility data for each channel and CLEANing them. The 256 line images were put into two data cubes, one for hydrogen and the other for carbon and heavy element lines. The average of the visibility functions for 82 channels (an equivalent bandwidth of  $0.25 \text{ MHz}$ ) free of the line in the hydrogen data cube was used to generate the continuum image of W48. Additional data reduction of the cubes for spatial distribution and velocity structure of the lines was performed using the Groningen Image Processing System (GIPSY; van der Hulst et al. 1992). For the main source, W48A, for each pixel, four Gaussian components were fitted to the line image channels of the hydrogen and carbon cubes; two components were fitted for the H<sup>+</sup> and H<sup>0</sup> profiles, two for the C<sup>+</sup> and the heavy element feature Z<sup>+</sup>.

### 3. RESULTS

Figure 1 shows the continuum image of the W48 H II region complex at  $\lambda 22 \text{ cm}$ . Observational parameters of the five H II regions, labeled A through E in the figure, are given in Table 1. The first column lists the source, the second and third columns

give  $\alpha$  and  $\delta$  which are the center coordinates of an elliptical Gaussian fit to the H II region, and the fourth column gives  $\Omega_c$ , the solid angle of the source that yielded the integrated continuum flux density. The fifth column lists  $S_c$  which is the integrated continuum flux density in janskys within the  $3\sigma$  noise contour of each source, and the sixth column gives the continuum emission measure calculated from the equation,

$$EM_c = \frac{T_c T_e^{*0.5} \nu^2}{3.01 \times 10^4 \ln(49.5 T_e^{*1.5} / \nu)} \quad (1)$$

(e.g., Onello et al. 1991), where  $\nu$  is the observing frequency in MHz,  $T_c = 3.85 \times 10^8 S_c / (\nu^2 \Omega_c)$  is the continuum temperature, and  $T_e^*$  is the electron temperature from Table 2 calculated assuming the lines are emitted in LTE. Column (7) lists  $\tau_c$ , the estimated continuum optical depth at  $1.4 \text{ GHz}$ .  $T_e^*$  is not listed in Table 2 for W48C since no H168 $\alpha$  line was detected from the source. We therefore have assumed an electron temperature of  $10^4 \text{ K}$  in computing the emission measure for the H II region. W48C is compact. If it is optically thick the assumption used to derive equation (1) is not valid.

We detected H168 $\alpha$  radio recombination lines from W48A, B, D, and E, and heavy element recombination lines (C168 $\alpha$  and Z168 $\alpha$ ) from W48A. Figure 2 shows the spectra we observed. Each profile is a spatial average with the spectrum from each map pixel weighted by the continuum intensity. The averaged line parameters are listed in Table 2. Columns (1)–(7) list the source name, the line transition, the velocity of the line centroid with respect to the local standard of rest ( $V_{lsr}$ ), the full width at half-maximum ( $\Delta V$ ), the line-to-continuum ratio ( $L/C$ ), the Doppler temperature ( $T_D$ ), and the electron temperature ( $T_e^*$ ).

The Doppler temperature is an upper limit to the kinetic temperature of the gas and is given by  $T_D = 21.8A(\Delta V)^2$ , where  $A$  is the atomic weight. It should be noted that the Doppler temperature of  $200 \text{ K}$  listed in Table 2 for the H<sup>0</sup> emission region in W48A represents one of the lowest temperatures ever observed for a Galactic H II region. Recently Phillips, Onello, & Kulkarni (1993) reported detecting an H<sup>0</sup> line emanating from cold gas of comparable temperature in the partially ionized region associated with the molecular globule G70.7+1.2.

<sup>3</sup> The Very Large Array of the National Radio Astronomy Observatory is operated by Associated Universities, Inc., under a cooperative agreement with the National Science Foundation.

TABLE 1  
W48 H II REGIONS

Source (1)	$\alpha$ (1950.0) (2)	$\delta$ (1950.0) (3)	$\Omega_c$ (arcmin <sup>2</sup> ) (4)	$S_c$ (Jy) (5)	$EM_e$ (pc cm <sup>-6</sup> ) (6)	$\tau_c$ (1.4 GHz) (7)
W48A .....	18 <sup>h</sup> 59 <sup>m</sup> 14 <sup>s</sup> .6	01°08'38"	21.1	12.8 ± 0.4	7.1 × 10 <sup>4</sup>	0.014
W48B .....	18 59 21.2	01 11 11	8.8	0.5 ± 0.1	5.4 × 10 <sup>3</sup>	0.002
W48C .....	18 59 43.1	01 18 00	4.0	0.27 ± 0.02	8.2 × 10 <sup>3</sup>	...
W48D .....	18 59 48.3	01 14 45	45.4	3.5 ± 0.2	7.6 × 10 <sup>3</sup>	0.003
W48E .....	18 58 15.0	01 08 30	98.8	3.3 ± 0.5	2.9 × 10 <sup>3</sup>	0.002

TABLE 2  
INTEGRATED LINE PARAMETERS

Source (1)	Line (2)	$V_{lsr}$ (km s <sup>-1</sup> ) (3)	$\Delta V$ (km s <sup>-1</sup> ) (4)	$L/C$ (5)	$T_D$ (K) (6)	$T_e^*$ (K) (7)
W48A .....	H168 $\alpha$ (H <sup>+</sup> )	45.2 ± 0.3	33.9 ± 0.6	0.78% ± 0.02%	25000	8800
	H168 $\alpha$ (H <sup>0</sup> )	43.4 ± 0.2	2.9 ± 0.6	0.24 ± 0.07	200	...
	C168 $\alpha$ (C <sup>+</sup> )	43.2 ± 0.1	3.0 ± 0.2	0.85 ± 0.07	2400	...
	Z168 $\alpha$ (Z <sup>+</sup> )	34.3 ± 0.1 <sup>a</sup>	2.4 ± 0.3	0.21 ± 0.04	4000	...
W48B .....	H168 $\alpha$	41.2 ± 1.6	21.5 ± 3.8	2.36 ± 0.57	10000	5000
W48D .....	H168 $\alpha$	46.7 ± 0.7	15.9 ± 1.5	2.88 ± 0.38	5500	5500
W48E .....	H168 $\alpha$	45.5 ± 0.6	18.7 ± 1.5	3.72 ± 0.47	7600	3800

<sup>a</sup> Value listed for the Z transition is on the velocity scale of C168 $\alpha$ .

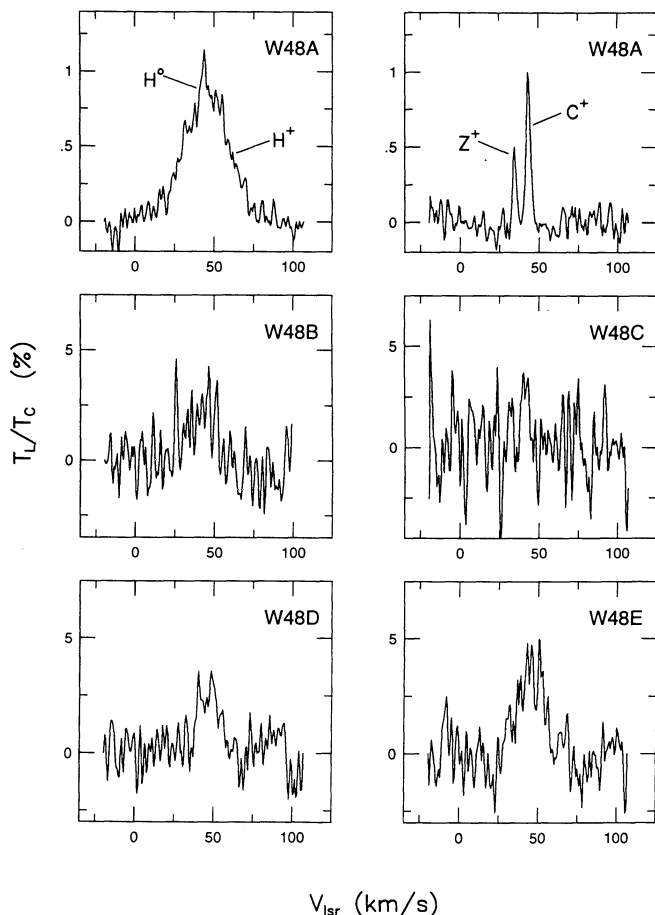


FIG. 2.—Integrated recombination line profiles

The thermal electron temperature was computed from the intensity of the H168 $\alpha$  line by using the expression (Brown 1987)

$$T_e^* = \{6.35 \times 10^3 v^{1.1} [(L/C)\Delta V]^{-1}\}^{0.87}, \quad (2)$$

where  $v$  is the line frequency in GHz,  $L/C$  the line-to-continuum temperature ratio, and we have assumed that hydrogen and helium were in their cosmic abundances. We do not list values of  $T_e^*$  for the H<sup>0</sup>, C<sup>+</sup>, and Z<sup>+</sup> because we could not measure the weak continuum emission from the partially ionized gas.

#### 4. DISCUSSION

W48 (G35.2–1.8) is located in a region of the sky with no optical nebula visible at its position. In Paper I the calculated value for the excitation parameter suggested that an O9 star was ionizing the gas. The authors interpreted the 168 $\alpha$  line profiles obtained with the single-dish Arecibo telescope in terms of the “blister” model (Israel 1978). In the model the exciting star is located near the edge of a dense molecular cloud, and as the H II region expands, one side pushes into the cloud, producing shock fronts which may be the site of star formation (Lada et al. 1978) while the other side flows into the more rarified interstellar medium. If the H II region is located between the observer and the dense molecular cloud, the blister model predicts that RRLs will be blueshifted with respect to the molecular lines because the H II nebula is expanding toward the observer and away from the molecular region. Conversely, if the molecular cloud is situated between the observer and the H II region, the RRLs will be redshifted with respect to the molecular lines.

Zeilik & Lada (1978) showed that the velocity of CO emission from gas around W48 coincided with the carbon recombination line velocity. We found in Paper I that the H<sup>0</sup> and C<sup>+</sup>



velocities are nearly identical and used kinematic arguments to suggest that the  $H^0$ ,  $C^+$ , and  $Z^+$  emission came from a partially ionized envelope around the hot fully ionized H II region. The velocity difference  $\Delta V(H\text{ II} - H^0)$  for W48 was found at Arecibo to be  $2.6 \pm 0.6 \text{ km s}^{-1}$ , in good agreement with the value of  $2.0 \pm 0.3 \text{ km s}^{-1}$  we found using the VLA. According to the blister model, the positive value indicates the H II region was behind the partially ionized gas and molecular cloud. We argued on that basis in Paper I that the strong  $H^0$  and  $C^+$  recombination lines in W48 resulted from stimulated amplification of the background radio source.

The results of the aperture synthesis imaging of W48A at the hydrogen and carbon  $168\alpha$  transitions are shown in the colored plate (Fig. 3 [Plate 4]). Figure 3A shows contours for the spatial distribution of the  $H^+$  integrated line intensity overlaid with a pseudo-color continuum image of W48A. The  $H^+$  line is most intense near, but not exactly at, the continuum peak of the H II region. The small offset could be due to temperature or density gradients inside the H II region (see, e.g., Roelfsema 1990).

Figures 3B and 3F show the  $C^+$  and  $Z^+$  line intensities overlaid on the W48A continuum. As can be seen, both lines are strongest at the continuum peak. Although the  $C^+$  line intensity contours extend over a slightly larger area than that of the  $Z^+$ , their similarity suggests that the region responsible for heavy element emission may be spatially coincident with the carbon emission region. As we discussed in § 1, the partially ionized carbon and sulfur are probably distributed in an extended zone around the H II region where photons with  $\lambda > 912 \text{ \AA}$  ionize gas outside the Strömgren sphere. If the RRL emission were spontaneous we would expect to see an extended distribution of  $C168\alpha$  and  $Z168\alpha$  larger than the H II region itself. Instead, we see that the line intensities are strongest in a limited region centered on the continuum peak of the H II region. This suggests that the recombination line intensities are enhanced by stimulated amplification of the background source.

Solutions of stimulated emission models for W48 (Silverglate & Terzian 1974) indicate the kinetic temperature of the  $C^+$  gas is comparable to the temperature of the  $H^0$  emission region. The Doppler temperatures we derived for the  $C^+$  and  $S^+$  gas are much larger than the temperature calculated from the  $H^0$  profile and can be explained by line widths dominated by turbulence. If line broadening arises primarily from the thermal motion of the gas, we would expect the line widths to be narrower for the more massive elements. In fact, we see that the  $H^0$ ,  $C^+$ , and  $S^+$  lines have comparable widths. The Doppler equation generalized to include turbulence is given by the expression

$$(\Delta V)^2 = (0.0458 T_e^*)1/A + 1.85 v_t^2, \quad (3)$$

where  $v_t$  is the rms of the turbulent component of the gas velocity in  $\text{km s}^{-1}$ . There are no values for  $T_e^*$  and  $v_t$  that will simultaneously give the observed line widths for all three lines. The observed line widths for carbon and sulfur are both consistent with lines emanating in a gas at 200 K with  $v_t \approx 2 \text{ km s}^{-1}$ . If the  $H^0$  line were broadened by the same amount of turbulence, then the kinetic temperature of the  $H^0$  gas would only be  $\approx 20 \text{ K}$ . Taken at face value this discrepancy suggests that the  $H^0$  emission region is physically distinct from that of the  $C^+$  and  $S^+$  gas.

Figures 3C and 3D show the velocity fields of the  $H^+$  and  $C^+$  lines overlaying the continuum contours. We obtained the

velocities by fitting a Gaussian to spectral lines in all pixels where the signal-to-noise ratio was greater than  $3\sigma$ . Velocity fields are not shown for the  $H^0$  and  $Z^+$  lines because the lines were only strong enough in a few pixels to measure the central velocities reliably. The velocity distributions of the  $H^+$  and  $C^+$  lines have a similar triangular appearance, but there is an offset of  $2 \text{ km s}^{-1}$  between the mean velocities of the two lines. The  $H^+$  velocities range from 41 to 49  $\text{km s}^{-1}$ , while the  $C^+$  emission is only found at velocities between 43 and 44  $\text{km s}^{-1}$ . The velocity difference is consistent with the idea that the ionized carbon lies in cold gas outside the expanding  $H^+$  region.

The spatial distribution of the  $H^0$  integrated line intensity is shown in Figure 3E. The  $H^0$  intensity peak and emitting region lie south of the H II continuum peak. Table 2 lists similar  $V_{\text{lsr}}$  values for the  $H^0$  and  $C^+$  lines, but Figures 3E and 3B show that the maxima in the  $H^0$  and  $C^+$  intensities are displaced from each other. Although there is some overlap, the overall distribution of the  $H^0$  line differs significantly from that of  $C^+$  and  $Z^+$  and provides further evidence that the  $H^0$  line emission originates in different gas. The limited spatial distribution of the  $H^0$  emission region would suggest that a shock produced in the advancing ionization front of the H II region, rather than soft X-rays in an extended stellar wind, is responsible for ionizing the cold 200 K gas. However, the difficulty in extracting the narrow  $H^0$  profile from the broad  $H^+$  emission feature and the lack of information on the kinematic structure of the  $H^0$  line in the source require that observations be made at different transitions to determine which of the two mechanisms is the ionizing source.

The data are consistent with a simple onion skin model in which cold hydrogen is ionized in a thin layer just outside the hot H II region (Hill 1977; Krügel & Tenorio-Tagle 1978) and cold carbon is ionized by photons with  $\lambda > 912 \text{ \AA}$  in a more extended C II zone. Although the C II zone may be physically larger than the  $H^0$  zone, we only see the stimulated RRL emission where the background continuum is strongest. The apparent sizes are therefore similar.

## 5. CONCLUSIONS

Using the D-configuration of the VLA, we have observed  $H168\alpha$  RRLs (1375 MHz) from four sources in the W48 H II region complex, and the narrow hydrogen feature  $H^0$  together with heavy element RRLs ( $C168\alpha$  and  $Z168\alpha$ ) from the partially ionized medium of W48A. High spatial resolution imaging of W48A revealed that both the  $C^+$  and  $Z^+$  lines are centered on the continuum peak, providing strong evidence that these lines arise from stimulated emission of the background H II region. Different line intensity distributions also revealed that the  $C^+$  and  $Z^+$  gas is not coextensive with the gas responsible for the  $H^0$  line. However, the observations are consistent with  $H^0$  emission emanating from a shocked, very cold ( $T \approx 200 \text{ K}$ ), partially ionized envelope around the hot, fully ionized gas in W48A.

J. S. O. would like to thank the National Radio Astronomy Observatory at Socorro, NM, for partial travel support and for the warm hospitality of the AOC staff. Y. T. wishes to thank the National Astronomy and Ionosphere Center, which is operated by Cornell University under a cooperative agreement with the NSF, and David F. Chernoff for useful discussions on interstellar shocks. We are grateful to the referee, Peter Roelfsema, for helpful comments and suggestions.



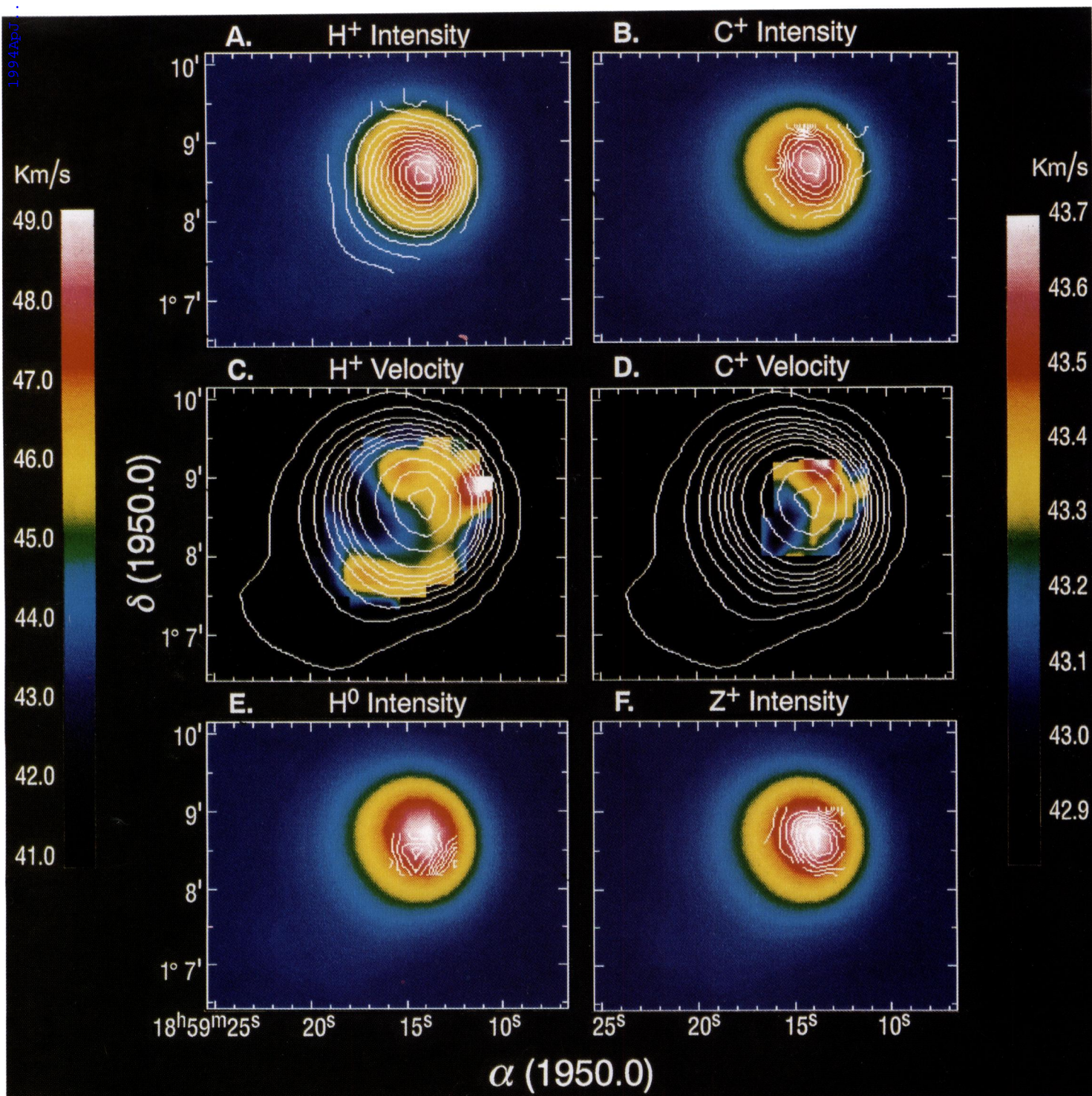


FIG. 3.—(A) H<sup>+</sup> integrated line intensity (contours) overlaid on a pseudo-color continuum image of W48A. The H<sup>+</sup> contours range from 5 to 49 mJy/beam in steps of 4.0 mJy/beam. (B) C<sup>+</sup> integrated line intensity (contours) overlaid on a pseudo-color continuum image of W48A. The contour levels range from 35 to 170 mJy/beam in steps of 15 mJy/beam. (C) H<sup>+</sup> velocity field (color) overlaid on a contour plot of the W48A continuum emission. Contour levels are 10, 30, 50, 75, 100, 125, 150 mJy/beam, 2, 3, 4, 5 Jy/beam. The velocity color bar is to the left of the figure. (D) C<sup>+</sup> velocity field (color) overlaid on a contour plot of the W48A continuum emission. Contour levels are the same as in Fig. 3C. The velocity color bar is to the right of the figure. (E) H<sup>0</sup> integrated line intensity (contours) overlaid on a pseudo-color continuum image of W48A. The contour levels range from 27 to 62 mJy/beam in steps of 7 mJy/beam. (F) Z<sup>+</sup> integrated line intensity (contours) overlaid on a pseudo-color continuum image of W48A. The contour levels range from 23 to 79 mJy/beam in steps of 7 mJy/beam.

ONELLO et al. (see 426, 252)

## REFERENCES

- Brown, R. L. 1987, in *Spectroscopy of Astrophysical Plasmas*, ed. A. Dalgarno & D. Layzer (Cambridge: Cambridge Univ. Press), 49
- Cornwell, T. J., Uson, J. M., & Haddad, N. 1992, *A&A*, 258, 583
- Gordon, M. A. 1988, in *Galactic and Extragalactic Radio Astronomy*, ed. G. L. Verschuur & K. I. Kellerman (Berlin: Springer), 88
- Hill, J. K. 1977, *ApJ*, 212, 692
- Israel, F. P. 1978, *A&A*, 70, 769
- Krügel, E., & Tenorio-Tagle, G. 1978, *A&A*, 70, 51
- Lada, C. J., Elmegreen, B. G., Cong, H., & Thaddeus, P. 1978, *ApJ*, 226, 39
- Onello, J. S., Phillips, J. A., & Terzian, Y. 1991, *ApJ*, 383, 693 (Paper I)
- Phillips, J. A., Onello, J. S., & Kulkarni, S. R. 1993, *ApJ*, 415, L143
- Roelfsema, P. R. 1990, in *Radio Recombination Lines: 25 Years of Investigation*, ed. M. A. Gordon & R. L. Sorochenko (Dordrecht: Kluwer), 39
- Silverglate, P. R. 1984, *ApJ*, 278, 604
- Silverglate, P. R., & Terzian, Y. 1978, *ApJ*, 224, 437
- van der Hulst, J. M., Terlouw, J. P., Begeman, K. G., Zwitter, W., & Roelfsema, P. R. 1992, *Astronomical Data Analyses Software and Systems I*, ed. D. M. Worrall, C. Biemesderfer, & J. Barnes (ASP Conf. Ser. 25), 131
- Zeilik, M., II, & Lada, C. J. 1978, *ApJ*, 222, 896